

Rethinking Class-incremental Learning in the Era of Large Pre-trained Models via Test-Time Adaptation

Imad Eddine Marouf¹Subhankar Roy²Stéphane Lathuilière¹Enzo Tartaglione¹¹LTCI, Télécom-Paris, Institut Polytechnique de Paris²University of Aberdeen

imad.marouf@ip-paris.fr

Abstract

Class-incremental learning (CIL) is a challenging task that involves sequentially learning to categorize classes from new tasks without forgetting previously learned information. The advent of large pre-trained models (PTMs) has fast-tracked the progress in CIL due to the highly transferable PTM representations, where tuning a small set of parameters leads to state-of-the-art performance when compared with the traditional CIL methods that are trained from scratch. However, repeated fine-tuning on each task destroys the rich representations of the PTMs and further leads to forgetting previous tasks. To strike a balance between the stability and plasticity of PTMs for CIL, we propose a novel perspective of eliminating training on every new task and instead train PTM only on the first task, and then refine its representation at inference time using test-time adaptation (TTA). Concretely, we propose **Test-Time Adaptation for Class-Incremental Learning (TTACIL)** that first fine-tunes PTMs using Adapters on the first task, then adjusts Layer Norm parameters of the PTM on each test instance for learning task-specific features, and finally resets them back to the adapted model to preserve stability. As a consequence, our TTACIL does not undergo any forgetting, while benefiting each task with the rich PTM features. Additionally, by design, our TTACIL is robust to common data corruptions. Our method outperforms several state-of-the-art CIL methods when evaluated on multiple CIL benchmarks under both clean and corrupted data. Code is available at: <https://github.com/IemProg/TTACIL>

1. Introduction

Deep learning has led to remarkable progress in various computer tasks, namely image classification [15, 22], object detection [70] and semantic segmentation [33]. Much of the success can be attributed to the broad availability of

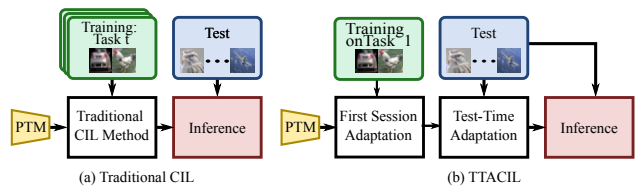


Figure 1. Comparison of traditional CIL methods with our TTACIL. (a) Traditional CIL methods entail training on each task’s training data, making it prone to forgetting. (b) In TTACIL, we train the PTM only on the first task using Adapters, then adjust its representations for the subsequent tasks using Test-Time Adaptation. After inference, the model is reset back to the adapted PTM: this ensures a better *stability-plasticity* trade-off.

offline data that are used for training on a set of limited classes. However, in many real-world scenarios, learning occurs continuously on incoming data streams that often introduce new classes [20]. As a consequence of the sequential updates of the network on the new classes, it leads to a phenomenon known as *catastrophic forgetting* (CF) [19], where previously acquired knowledge is erased in favor of the new one. To address this challenge, Class-Incremental Learning (CIL) has been introduced: it enables models to learn new classes continually from evolving data, which are stored temporarily, without losing the ability to classify previous classes while using a unified classifier [47].

The status quo in the CIL literature entails training the network (typically ResNets [22]) from scratch on the data from the current session (or *task*), alongside optimizing a regularization objective for mitigating forgetting [47, 74]. Recently, with the rise of the generalist and expressive Vision Transformer (ViT) based [15] pre-trained models (PTMs), trained on large datasets (*e.g.* ImageNet [13]), leveraging the PTMs for the incremental tasks has emerged as a viable alternative [71, 76–78, 89] in CIL. Using PTMs significantly enhances the data efficiency of CIL and consis-

tently outperforms the traditional CIL methods trained from scratch [88]. For instance, Zhou *et al.* [89] demonstrated that adopting the nearest class mean (NCM) [48] classification approach using a frozen PTM leads to competitive performance, surprisingly outperforming several state-of-the-art CIL approaches. This simple yet strong baseline reaffirms the generalizability of PTMs for CIL.

Although frozen PTMs attain impressive performance in CIL, such an approach suffers from *intransigence*, which is characterized by a lack of freedom to learn new tasks [9]. To remedy this issue, trending CIL methods rely on parameter efficient tuning, such as prompt-tuning [77, 78] or fine-tuning adapters [55, 89], while keeping PTM weights frozen. In particular, the CIL methods “ADapt And Merge” (ADAM) [89], and FSA [55] employ *first session adaptation*, where the PTM is fine-tuned *only* on the first task, among the sequences of all the tasks in a dataset, to adapt to the dataset at hand. While fine-tuning only on the first task is proven to be a strong baseline for CIL, *it still can not fully adapt to the whole dataset containing very heterogeneous tasks* (see Sec. 4.3 for an empirical study). Any attempt to achieve full plasticity by sequential fine-tuning on all tasks results in poor stability due to CF.

In this work, we offer an alternative perspective to better address the stability-plasticity dilemma. With the goal of achieving continued plasticity after the first session adaptation (through Adapters [11]), we propose to refine the representation of the PTM after the first task with test-time adaptation (TTA) [84] on each test instance (see Fig. 1). TTA, which was originally conceived for mitigating *domain shift* [60] between a pre-trained source model and the unlabelled data in the target domain [39], *satisfies two important desiderata in CIL: (i) plasticity* by fine-tuning only a small subset of parameters (*e.g.*, Layer Norm [3]) of the PTM on the unlabelled test instance to adapt to any new task at hand; *(ii) stability* by resetting the model back to the post first session adaptation PTM checkpoint. Unique to our proposed method, it preserves the generalizable representation power of the PTM, while being malleable enough to learn new tasks, unlike in [55, 89]. We therefore call our method as **T**est-**T**ime **A**daptation for **C**lass-**I**ncremental **L**earning (or TTACIL). Note that the *goal of this work is neither to propose a novel method for TTA, nor to propose a new setting for CIL, but to demonstrate that TTA is a promising solution for effective CIL in the era of large PTMs.*

More formally, our TTACIL is composed of two phases. In **Phase I**, similarly to ADAM, we fine-tune randomly initialized adapters on the first task’s training data to learn task-specific and *loosely* dataset-specific features (see Sec. 3.3). Note that first-session adaptation does not aid in forgetting, given that forgetting occurs during sequential parameter updating. In **Phase II**, we perform TTA directly on the unlabelled test instances of each task by unlocking ex-

clusively the learnable parameters of Layer Normalization (see Sec. 3.4). This allows the network to adapt to the intricate task-specific features from subsequent tasks, while not deviating too far from the generalizable adapted PTM representations of Phase I. As a TTA objective, we minimize the entropy of the marginal distribution of the model predictions on augmented versions of a given test sample [84]. In practice, we find that only a single adaptation step (or gradient update) is sufficient to reach good performance without incurring higher computation costs at inference. After adaptation on each sample, we reset the model back to the base model in Phase I to ensure stability. We will empirically demonstrate that TTACIL achieves state-of-the-art results on CIL benchmarks via TTA and model resetting (see Sec. 4.2), thereby questioning the utility of continuous model updates which is prevalent in the CIL literature.

The novel perspective of addressing CIL with TTACIL presents several **benefits**: **(i)** it cuts computation during training time by limiting the training to just the first task; **(ii)** it does not lead to irreversible forgetting on the previous tasks as the model is reset after every adaptation on a new sample, hence capitalizing the strong generalizability of PTMs; **(iii)** it is robust to unforeseen alterations to test samples, such as synthetic corruptions and perturbations [24], a critical aspect which has been overlooked in CIL; **(iv)** it is highly parameter-efficient while being state-of-the-art in many CIL benchmarks. Unlike many CIL methods, our TTACIL is intuitive and simple to implement.

In summary, our **contributions** are the following: **(i)** we bring a paradigm shift in CIL with our proposed TTACIL by successfully demonstrating that TTA is a potent and efficient solution for CIL in the era of large PTMs; **(ii)** we are the first to highlight the need to evaluate the robustness of CIL methods against common corruptions - TTACIL is implicitly robust to such corruptions; **(iii)** we extensively benchmark PTM-based CIL methods, including benchmarks that have large domain gaps with the pre-training data: our TTACIL outperforms state-of-the-art CIL methods on both clean and corrupted data.

2. Related Work

Class-Incremental Learning. CIL is an active area of research (see the surveys in [5, 47, 56, 74]) that deals with incrementally expanding the knowledge of a model to recognize new classes by training on labeled data arriving in sessions. While learning the new classes the model tends to forget previously acquired information due to the phenomenon called catastrophic forgetting [19]. Therefore, the CIL methods aim at simultaneously balancing the knowledge acquisition (*i.e.*, *plasticity*) and the knowledge retention (*i.e.*, *stability*) capabilities of the model [49].

The CIL methods can be broadly categorized into four distinct groups. (i) Weight regularization CIL methods [2,

9, 34, 37, 40, 81] aim at preventing a drift in the weights of the network which are relevant to the previous tasks. (ii) Data regularization CIL methods [8, 14, 16, 28, 32, 38, 41, 62] instead aim at preventing drift in the network activation by employing knowledge distillation [27]. (iii) Memory rehearsal CIL methods reduce forgetting by storing and replaying a small number of exemplars [6, 8, 58, 62], or by generating synthetic images [54, 66] or features [80]. (iv) Architecture growing CIL methods [44, 45, 64, 65] that dynamically increase the capacity of the network through allocating task-specific learnable parameters to prevent interference between tasks, and hence reduce forgetting. Our proposed TTACIL is unique from most of the existing CIL literature as it operates directly at test-time. Although similar in spirit with GDumb [58], which re-trains the network at test-time from scratch using exemplars from the memory, our TTACIL is *rehearsal-free* and requires only a single gradient update on the test sample to be ready for inference. Furthermore, TTACIL trains solely on the initial task, avoiding overfitting to new classes.

CIL with Large Pre-Trained Models. With the introduction of large PTMs [15] the field of CIL has seen a rapid progress [67, 77, 78, 83, 89, 90]. It is mainly driven by the fact that PTMs are highly generalizable to downstream tasks and tuning only a small subset of parameters is sufficient to obtain good performance [11, 29, 46]. Broadly speaking, all the PTM-based CIL methods can be classified under two categories. The *first* category consists of prompt-tuning [31] based CIL methods [67, 71, 77, 78] that keep the PTM frozen and aim to train a set of learnable tokens (or prompts) on the training data to learn task-specific features. At inference, they query the prompt pool to retrieve a prompt on the test instance, then condition the frozen PTM with the selected prompt. The *second* category consists of CIL methods that compute class means using frozen PTM features and use NCM classifier to classify test samples [30, 55, 89]. Entirely frozen PTM being restrictive [30], FSA [55] and ADAM [89] attempt to improve plasticity by adapting the PTM on the first task data. From the second task onwards the PTM is kept frozen. Differently from the prior works, our TTACIL encourages plasticity beyond the first task via test-time adaptation.

Test-Time Adaptation. TTA has been proposed to improve the performance of a PTM (trained on *source* data) on out-of-distribution test (or *target*) data, exhibiting domain-shift, by adjusting the model parameters using the unlabelled test samples [4, 10, 39, 42, 69, 73, 84]. In particular, the covariate shift is simulated with synthetic corruptions [24] (e.g. Gaussian noise, blur, shot noise) or natural shifts (e.g. sim to real [57]). Typically TTA methods optimize an unsupervised loss (e.g. entropy minimization [21]) using the test instance and update either all the parameters of the network [84] or only a subset (e.g. Batch Normalization lay-

ers [73]). Post adaptation, the resulting model is used for inference on the test instance, after which it is either reset back to the original checkpoint [84] or directly used for the next adaptation steps [73].

Differently from the original motivation of TTA – to reduce domain shift between the train and *corrupted* test sets sharing the *same label space* – TTACIL exploits the generalizable PTM features to adapt from pre-training datasets to downstream task datasets having potentially *disjoint* labels. Moreover, CIL is also different from Continual TTA [68, 75], where the latter considers each task as a different kind of corruption but under the same label space, while in CIL the label space evolves with each task.

3. Proposed Framework

In this section, we introduce the setting of CIL, then we define our method that addresses the main challenges of CIL.

3.1. Problem Formulation

CIL involves learning from a data stream that introduces new classes and aims to construct a unified classifier [62]. The training process consists of a sequence of T training tasks, denoted as $\mathcal{D} = \{\mathcal{D}^1, \mathcal{D}^2, \dots, \mathcal{D}^T\}$ with incremental data \mathcal{D}^t for each new task, each composed of K^t classes; hence, we have $K = \sum_{t=1}^T K^t$ total number of classes. For each class k , the number of training samples is N_k .

In this context, \mathbf{x}_i refers to a training instance belonging to the class $y_i \in Y^t$, where Y^t is the label space of task t . In our case, there is no overlap in the label spaces between different tasks, i.e., $Y^t \cap Y^{t'} = \emptyset$ for $t \neq t'$. During the t -th training stage, only data from \mathcal{D}^t can be accessed for model updates. Following the approach as in [77, 78], we assume the availability of a PTM, such as a ViT [15] trained on the ImageNet-21K dataset [63]. This pre-trained model serves as the initialization for the CIL model. A successful CIL model f acquires knowledge from new classes while preserving it from the previously encountered ones. The evaluation of the model’s capability is performed across all seen classes, denoted as $\mathcal{Y}^T = Y^1 \cup \dots \cup Y^{t-1} \cup Y^t$, after each incremental task t .

3.2. Baseline: Prototype-classifier with PTMs

Inspired by [48, 62], we employ an approach called “Prototype-Classifier” (PC) to transfer PTM knowledge for incremental tasks. We denote E_θ as the features extractor of the PTM model f , having θ as its parameters. We employ E_θ to estimate the class prototypes \mathbf{c}_k , with $k = 1, \dots, K$. To achieve this, we freeze the embedding function E_θ and compute the average embedding for each class in the current task \mathcal{D}^t as

$$\mathbf{c}_k = \frac{1}{N_k} \sum_{j=1}^{|\mathcal{D}^t|} \delta_{y_j, k} E_\theta(\mathbf{x}_j), \quad (1)$$

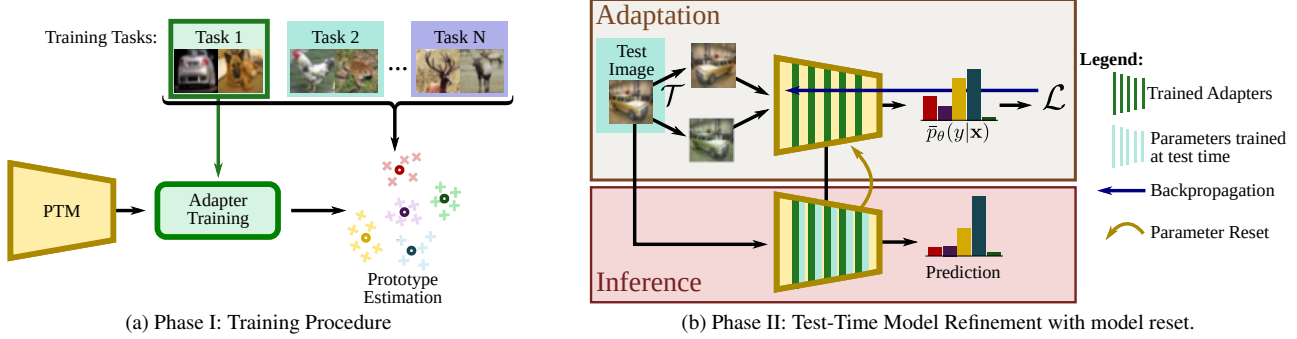


Figure 2. Our TTACIL is composed of two phases. In **Phase I**, we fine-tune adapters [11] with parameters ϕ on the first task’s training data to learn task-specific features. In **Phase II**, we perform model refinement at test-time directly on the unlabelled test instances of each task. This allows the network to adapt to the intricate task-specific features from subsequent tasks, while not deviating too far from the generalizable PTM representations.

where $\delta_{a,b}$ is the Kronecker delta. The averaged embedding c_k aims at capturing the most common pattern observed in each class. For a test instance \mathbf{x}_i , we estimate the probability of each class k via the dot products between the image feature representation $\mathbf{z}_i = E_\theta(\mathbf{x}_i)$ and each prototype through:

$$p_\theta(y_i = k | \mathbf{z}_i) = \frac{\exp(\mathbf{z}_i \cdot \mathbf{c}_k)}{\sum_j \exp(\mathbf{z}_i \cdot \mathbf{c}_j)}. \quad (2)$$

In our case, the CIL model f includes the feature extractor E_θ and the prototype classifiers. Our experiments show that PCs can achieve competitive performance even without fine-tuning on the target dataset (refer to Sec. 4.2). However, when the downstream datasets exhibit a domain shift compared to the dataset used for model pre-training, the performance drops. Such drop is evident especially when the new data demands specific domain insights or shows significant concept drift [1, 26].

To address this issue, we proceed in two adaptation phases: *Adapting PTMs to First Task*, followed by *Test-Time Model Refinement*. An overview of TTACIL is displayed in Fig. 2 and summarized in Algorithm 1.

3.3. Phase I: Adapting PTMs to First Task

To allow a certain level of plasticity, we employ an adaptation process, given that repeated adaptations to each new incremental task both trigger CF and weaken generalization [36]. To counter these, our approach performs feature adaptation primarily during the first task, and for the following tasks, the feature representation remains unchanged: this ensures that the model acquires domain-relevant insights early on without forgetting.

In the first task, we adapt E_θ by inserting lightweight modules inside each layer called Adapters [11]. The adapter parameters, denoted as ϕ , are learned on \mathcal{D}^1 , while the parameters θ of E_θ remain frozen. The adaptation is done by

minimizing a Cross-Entropy loss using stochastic gradient descent. Importantly, the parameters ϕ represent a tiny proportion of the total number of parameters in $E_{\theta,\phi}$ (about 1% – 3%) to prevent over-fitting on \mathcal{D}^1 .

This procedure provides an adapted features extractor $E_{\theta,\phi}^*$ encoding domain-specific knowledge.

3.4. Phase II: Test-Time Model Refinement

After the initial adaptation on the first task, we will obtain the prototypes for the new tasks from the adapted $E_{\theta,\phi}$. However, our model may still provide unsatisfactory results when it encounters visual content different from the past tasks; and any learning on all tasks carries a high risk of CF, creating risks of task-recency bias [43]. To tackle this, we propose to employ Test-Time Adaptation (TTA) which enables plasticity without suffering from CF. This TTA phase consists of a slight feature adaptation on the test images in an unsupervised fashion. After evaluation on each test batch, our model is reset to the initial adapted state $E_{\theta,\phi}^*$ (from Phase I) to maintain generability, and we prevent forgetting [18, 84]. An additional reason for adopting TTA is that it enhances the robustness of our model against noisy and corrupted samples during inference [69, 73].

Given a test sample \mathbf{x}_i , an adapted PTM model $E_{\theta,\phi}^*$ (from Phase I), and a set of image Transformations \mathcal{T} , we sample M random transformations $\{\tau_1, \dots, \tau_M\}$ from \mathcal{T} and apply them to \mathbf{x}_i to produce a batch of augmented data $\{\tilde{\mathbf{x}}_{i,1}, \dots, \tilde{\mathbf{x}}_{i,M}\}$. The marginal output distribution for the augmented points is given by:

$$\bar{p}_{\theta,\phi}(y | \mathbf{x}_i) \approx \frac{1}{M} \sum_{m=1}^M p_{\theta,\phi}(y | \tilde{\mathbf{x}}_{i,m}). \quad (3)$$

We propose to adapt the model by minimizing the entropy of its marginal output distribution over augmenta-

Algorithm 1 The pipeline of proposed TTACIL.

Require: Sequence of T tasks, $D = D^1, \dots, D^T$, and pre-trained model f

- 1: **Phase I:** *Adapting PTMs to New Tasks*
 - 2: Adapt model f using Adapters on D^1 .
 - 3: **Phase II:** *Test-Time Model Refinement*
 - 4: **for** a batch X in D_{test}^t **do**
 - 5: **Reset** the model to the initial state $f_{\theta, \phi}$.
 - 6: **for** iteration $n = 1 \dots N$ **do**
 - 7: Sample transformations from \mathcal{T} and apply to X .
 - 8: Calculate predictions via equation 3.
 - 9: Adapt parameters via equation 4.
 - 10: **end for**
 - 11: **end for**
 - 12: **return** predictions for all $\mathbf{x}_i \in D_{\text{test}}^t$.
-

tions (equation 3):

$$\mathcal{L}(\theta, \phi; \mathbf{x}_i) = - \sum_{y \in \mathcal{Y}} \bar{p}_{\theta, \phi}(y|\mathbf{x}_i) \log \bar{p}_{\theta, \phi}(y|\mathbf{x}_i). \quad (4)$$

In the process of minimizing equation 4, the model is driven to achieve both high confidence and invariance to input augmentations. Specifically, the entropy term $\bar{p}_{\theta, \phi}(\cdot|\mathbf{x}_i)$ reaches its minimum value when the model delivers consistent and confident predictions, regardless of the particular data augmentation applied. The motivation for optimizing the model to yield more confident predictions is grounded in the belief that the decision boundaries distinguishing classes are situated in areas of the data space with lower density [21, 84].

As $\bar{p}_{\theta, \phi}(y|\mathbf{x}_i)$ is differentiable with respect to the parameters (θ, ϕ) based on the loss defined in equation 4, we can employ gradient-based optimization directly to adapt parameters (θ, ϕ) . TTA requires careful selection of parameters [52], our adaptation procedure focuses solely on adapting the *layer-norm* parameters [3], unlike MEMO [84] which finetunes all the model. We found that adapting all the parameters hurts the performance (see Sec. 4.3). Only one iteration step per test point is empirically determined to be sufficient for achieving improved performance, with less inference time overhead. Then, we utilize the adapted model f' to make predictions on the test input \mathbf{x}_i .

4. Experiments

4.1. Experimental setup

Datasets and settings. We validate TTACIL on seven CIL benchmarks. In detail, following the work in [89] we experiment with CIFAR100 [35], CUB200 [72], ImageNet-R [25], ImageNet-A [26], OmniBench [85], 5-Datasets [78] and VTAB [89]. All these benchmarks offer diverse levels of difficulty in terms of high task heterogeneity (*e.g.*

5-Datasets, VTAB) or large domain gap to ImageNet (*e.g.* ImageNet-A). For the experiments on robustness, we pick three benchmarks: CIFAR100-C [24], OmniBench-C, and VTAB-C, where ‘‘C’’ stands for corrupted counterparts of the original benchmarks. In this work, we introduce the VTAB-C and OmniBench-C by adding the same corruptions as in CIFAR100-C to the original testing sets of VTAB and OmniBench benchmarks, respectively.

We follow the incremental settings established in [89], *i.e.* by adopting an increment per task of three types: 5 classes (Inc5) for CIFAR100 and ImageNet-R; 10 classes (Inc10) for CUB200, ImageNet-A, VTAB, and 5-Datasets; and 30 classes (Inc30) for OmniBench. The same increments and task orders are followed in the robustness experiments. Finally, we evaluate all the methods in *task-agnostic* manner, *i.e.* without having access to the task-id at inference. More details are available in the Supp. Mat.

Implementation details. Following ADAM [89], we have used ViT-B/16 [15] initially pre-trained on ImageNet-21K and further fine-tuned on ImageNet-1K, as a backbone. For Phase I, we trained the adapters (one adapter per ViT block) using Stochastic Gradient Descent (SGD) with momentum for 20 epochs, with an initial learning rate of 0.01 that undergoes cosine annealing. In Phase II we have used a batch size of 16 and augmented each test sample 8 times using random image transformations [84]. As mentioned before, for one mini-batch we do one gradient step in Phase II to obtain the adapted model. The learning rate is set to 0.01 and no weight decay is employed.

Baselines and competitors. We have compared our proposed TTACIL with the competitor PTM-based CIL methods that are state-of-the-art: **LwF** [34], **L2P** [78], **DualPrompt** [77], **ADAM**[89], **FSA-FiLM** [55] and **SLCA** [83]. All methods are initialized with the same PTM (ViT-B-16 [15]) pre-trained on Imagenet-21K. Additionally, we have compared with two more baselines: **Finetune** and **Finetune Adapter** [11].

Evaluation Metrics. In alignment with Rebuffi *et al.* [62], we denote the Top-1 accuracy achieved at the end of the t -th task as \mathcal{A}_t . We employ two key performance indicators: (i) \mathcal{A}_T , representing the Top-1 accuracy after learning the final task, and (ii) $\bar{\mathcal{A}}$, calculated as the average Top-1 accuracy while learning progresses in incremental steps.

4.2. Main results

Results on standard CIL benchmarks. We report in Tab. 1 the empirical evaluation on the standard CIL benchmarks, where we compare our proposed TTACIL with all the competitors. From the table, it is evident that TTACIL performs truly well, with an average accuracy $\bar{\mathcal{A}}$ of 83.17% which is the highest amongst all of the competitor methods. In some benchmarks such as CIFAR100 and CUB200, our TTACIL is the second best. Notably, except in CUB200,

Table 1. Average ($\bar{\mathcal{A}}$) and last performance (\mathcal{A}_T) comparison on six datasets with **ViT-B/16-IN21K** backbone. “IN-R/A” stands for “ImageNet-R/A”, and “OmniBench” stands for “OmniBenchmark”. LwF, L2P, and DualPrompt results are from [89]. † indicates results reported in the original paper. The best performance is in bold, and the second best is underlined.

Method	CIFAR100-Inc5		CUB-Inc10		IN-R-Inc5		IN-A-Inc10		OmniBench-Inc30		VTAB-Inc10		Average
	$\bar{\mathcal{A}}$	\mathcal{A}_T	$\bar{\mathcal{A}}$										
Finetune	38.90	20.17	26.08	13.96	21.61	10.79	21.60	10.96	23.61	10.57	34.95	21.25	27.79
Finetune Adapter [11]	60.51	49.32	66.84	52.99	47.59	40.28	43.05	37.66	62.32	50.53	48.91	45.12	54.87
LwF [38]	46.29	41.07	48.97	32.03	39.93	26.47	35.39	23.83	47.14	33.95	40.48	27.54	43.03
L2P [78]	85.94	79.93	67.05	56.25	66.53	59.22	47.16	38.48	73.36	64.69	77.11	77.10	69.53
DualPrompt [77]	87.87	81.15	77.47	66.54	63.31	55.22	52.56	42.68	73.92	65.52	83.36	81.23	73.08
Prototype-Classifier	86.27	81.27	90.79	86.77	61.63	54.33	58.66	48.52	80.63	73.33	85.99	84.44	77.33
FSA-FiLM [55]	90.13	86.23	<u>91.23</u>	86.12	73.65	65.13	60.11	49.53	80.64	74.09	87.47	82.12	80.53
ADAM † [89]	90.65	85.15	92.21	86.73	72.35	64.33	60.53	49.57	<u>80.75</u>	<u>74.37</u>	85.95	84.35	80.41
ADAM [89]	90.87	85.15	91.06	86.73	72.35	64.33	60.21	49.57	79.70	55.24	85.95	84.35	80.02
SLCA [83]	94.54	91.19	84.70	81.76	<u>74.10</u>	<u>69.73</u>	<u>61.98</u>	56.48	80.40	72.05	88.92	82.65	<u>80.77</u>
TTACIL (w/o Phase I)	85.48	81.04	90.56	86.85	61.76	54.42	58.62	48.65	80.65	73.30	<u>90.63</u>	<u>85.88</u>	77.95
TTACIL	<u>91.88</u>	<u>88.37</u>	91.21	<u>86.81</u>	78.24	69.95	65.67	<u>56.10</u>	81.13	76.39	90.94	86.90	83.17

Table 2. Average performance ($\bar{\mathcal{A}}$) comparison with **ViT-B/16-IN21K** as the backbone on three corrupted benchmarks CIFAR100-C, VTAB-C and OmniBench-C with Level-5 noise corruptions [24]. The best performance is in bold, and the second best is underlined.

Method	CIFAR100-C				VTAB-C				OmniBench-C			
	Gauss.	Shot	Impul.	Avg.	Gauss.	Shot	Impul.	Avg.	Gauss.	Shot	Impul.	Avg.
Prototype-Classifier	35.52	39.05	46.89	40.48	69.64	72.31	58.18	66.71	77.44	78.43	75.07	76.98
ADAM [89]	37.52	48.73	65.03	<u>50.43</u>	71.10	74.11	58.98	<u>68.06</u>	79.45	79.57	77.76	<u>78.93</u>
TTACIL	47.33	51.45	67.89	55.56	71.58	74.23	59.44	68.42	79.66	79.59	78.54	79.26

our TTACIL consistently outperforms ADAM [89] on all the benchmarks. This highlights that adaptivity is indeed important for learning task-specific features on each task. If training is limited to the first task, as done in ADAM, it leads to a drop of 3.38% in the average performance (80.02% vs 83.17%). Contrarily, if the adapters are fine-tuned on each task, as denoted by the Finetune Adapter baseline in Tab. 1, the final performance drops drastically to 52.87%, because fine-tuning has major downsides as mentioned in the Sec. 1. Contrarily, TTACIL allows plasticity while not running into severe forgetting after adapting to each test sample due to model reset.

Although our TTACIL w/o Phase I, as reported in Tab. 1, lags behind some state-of-the-art methods by some points, it still improves over Prototype-Classifier by +0.63%. This again highlights that the frozen PTMs are sub-optimal when it comes to datasets with data distribution different from the pre-training datasets. For instance, in the VTAB benchmark our TTACIL w/o Phase I achieves an improvement of +4.64% over PC that uses only frozen PTM features. Despite the simplicity, our TTACIL (and TTACIL w/o Phase I) outperforms all very complex prompt-tuning methods such as L2P and DualPrompt by several points on average.

Results on CIL benchmarks with corruptions. In Tab. 2 we report the empirical evaluation on CIL benchmarks with

different kinds of noise corruptions (of level 5 [24]), where we compare our proposed TTACIL with the competitors. In ADAM and our TTACIL, *we exclude training on the clean samples from every task, except the first task*. The Prototype-Classifier exhibits the worst performance as it solely relies on the representation learned from the pre-training dataset. ADAM, which trains the network on the training data from the first task, shows an improvement in performance due to better adaptivity to the PC. TTACIL achieves the best performance as it further allows the model to adapt towards every subsequent task. In particular, the gain in performance is significant for CIFAR100-C, where our proposed TTACIL outperforms ADAM by +5.13%.

In summary, our proposed TTACIL satisfies three desiderata: (i) improved adaptivity to new tasks; (ii) less computational cost by avoiding sequential training on each task; and (iii) robustness to corruptions by refining its predictions on the corrupted test instances during test-time. We report the results on other types of corruption in the Supp. Mat.

4.3. Ablation analysis

① **Effect of task ordering.** In Fig. 3 we study the influence of task order, especially in the case of heterogeneous tasks. We choose to perform experiments on the 5-

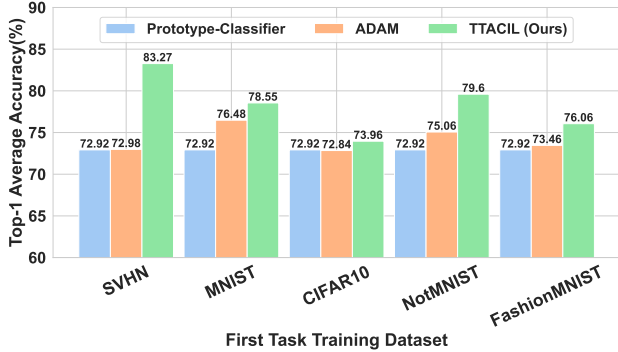


Figure 3. Comparative performance analysis of Prototype-Classifier, ADAM and our TTACIL when subjected to different task orderings. The first training task is indicated on the x-axis. Y-axis corresponds to the average performance across the datasets.

Datasets benchmark [77] as it contains five very heterogeneous datasets: SVHN, MNIST, CIFAR10, NotMNIST, and FashionMNIST. Here we mainly compare TTACIL with ADAM as both undergo training on the first task’s data.

From Fig. 3, we notice that a different task order yields different performance for TTACIL and ADAM, indicating that the first task plays an important role in determining the final performance. However, in all the task orderings, TTACIL outperforms ADAM by big margins, with the highest margin (+10.29%) obtained in the tasks of order SVHN \rightarrow MNIST \rightarrow CIFAR10 \rightarrow NotMNIST \rightarrow FashionMNIST. This highlights that the data from the second task onwards, despite *unlabelled*, offer a learning signal that is efficiently exploited by our TTACIL during Phase II. Differently, as ADAM does not offer any plasticity after the first task, it fails to improve the adaptivity on future tasks.

We can also observe that when the first task is CIFAR10, a dataset very different from the other tasks, TTACIL still yields a performance gain over both ADAM and Prototype-Classifier. These results are promising since they indicate that TTACIL is a relevant solution even when the domain shifts in future tasks are potentially large [59].

② Effect of the adaptation parameters. The experiments presented in Tab. 3 focus on evaluating different parameters to adapt, and the effect of model resetting during *Test-Time Model Refinement phase*. We compare: (i) *no TTA* – we do not apply test-time adaptation (equivalent to ADAM [89]); (ii) *All* – we adapt all the parameters of the model; (iii) *Adapter* – we adapt only the parameters of the adapter; and (iv) *Norm* – we adapt only the Layer Norm parameters.

Adapting all the parameters results in 87M trainable parameters, yielding lower VTAB and Imagenet-R accuracies of 43.26% and 26.02% respectively, likely due to the inherent complexity of adapting with few samples, and to one optimization iteration. The adapter-only update reduces train-

Table 3. Evaluation of different parameters subject to optimization during test-time used in TTACIL. Average performance (\bar{A}) is reported for VTAB and Imagenet-R (higher is better \uparrow). Number of trainable parameters in Million (M) (lower is better \downarrow).

		# of Par. (M) \downarrow	VTAB \uparrow	Imagenet-R \uparrow
TTA	No TTA	0	85.68 \pm 2.44	72.35 \pm 1.11
	All	87	43.26 \pm 1.15	26.02 \pm 0.39
	Adapter	1.2	89.89 \pm 0.64	75.28 \pm 0.97
	Norm	0.04	90.94 \pm 0.64	78.24 \pm 1.02

Table 4. Evaluation of different test-time adaptation approaches used in TTACIL. Average performance (\bar{A}) is reported for VTAB and Imagenet-A (higher is better \uparrow).

Method	VTAB \uparrow	Imagenet-A \uparrow
No-reset	43.31 \pm 7.34	41.77 \pm 9.29
TENT [73]	81.21 \pm 0.87	61.40 \pm 0.70
MEMO [84]	90.94 \pm 0.64	65.67 \pm 1.02
SAR [53]	83.79 \pm 1.15	55.69 \pm 1.92

able parameters to 1.2M, improving VTAB and Imagenet-R accuracies to 89.89% and 75.28%. The most efficient performance is achieved by updating only 0.04M Layer Norm parameters, aligning with Niu *et al.*’s [53] findings on norm-layer adaptations enhancing stability in TTA.

③ Effect of TTA approach. Our analysis proposed in Tab. 4 focuses on the effectiveness of different TTA methods—specifically TENT [73], MEMO [84], and SAR [53]—while constraining fine-tuning to layer-norm [3]. The analysis of different TTA methods within TTACIL highlights different performances: MEMO outperforms TENT and SAR with the highest average accuracies on VTAB (90.52%) and Imagenet-A (65.67%), exhibiting minimal variation across trials. Conversely, SAR shows an advantage over TENT on VTAB, indicating a higher variability in performance. The findings indicate that TENT and SAR’s effectiveness are sensitive to dataset specifics and task requirements [86].

The non-resetting approach yields sub-optimal results with high variance, indicating batch overfitting and potential knowledge loss from previous batches. Model resetting is necessary to mitigate batch sequence dependencies [86].

④ Effect of the PTM backbone. Here we evaluate, on VTAB, the influence of pre-trained models (PTMs). The analysis in in Fig. 4 incorporates PTMs such as ViT-B/16-IN1K/21K, ViT-B/16-DINO [7], ViT-B/16-SAM [12], ViT-B/16-MAE [23], and ViT-B/16-CLIP [61] (image encoder).

ViTs trained with supervised loss demonstrate enhanced performance over unsupervised counterparts. CLIP’s per-

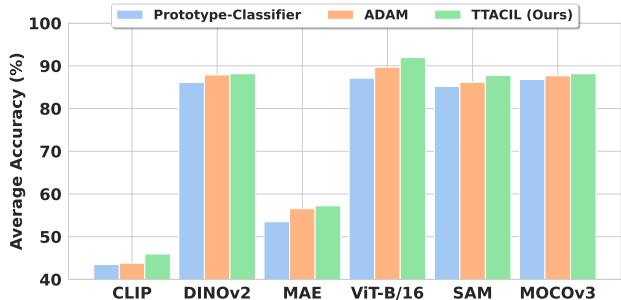


Figure 4. Evaluation of TTACIL with different PTMs on VTAB dataset. TTACIL consistently improves the performance of ADAM and Prototype-Classifier.

formance on the VTAB benchmark is the lowest, as indicated by Radford *et al.* [61]. CLIP features for VTAB dataset subsets show reduced discriminability, leading to lower performance compared to alternative backbones. Furthermore, the nature of the pre-training task contributes to MAE’s modest results on the VTAB benchmark. In summary, TTACIL surpasses ADAM across all backbones, attributed to the improvement during test-time adaptation.

⑤ Data Efficiency. As described in Sec. 3, training data is only used for prototype estimation (except for the first task) making our model potentially less prone to overfitting. However, the lack of plasticity could also induce difficulty in benefiting from large training sets. We analyze the performance of TTACIL considering training datasets of varying sizes. The results are visualized in Fig. 5.

First, we observe that with only 20% of the training data, TTACIL achieves a Top-1 accuracy of 88% on the VTAB dataset, compared to 87.01% by Prototype-Classifier and 86.89% by ADAM. The differences among baselines are smaller in the case of the Imagenet-R dataset. As the percentage of available training data increases, TTACIL’s advantage becomes even more prominent. At 60% of the training data, TTACIL registers an impressive 72% on Imagenet-R, whereas Prototype-Classifier and ADAM lag behind at 61.22% and 69.78%, respectively. Note that both ADAM and TTACIL use the same prototypes and undergo the same first task training. So, the performance gap is caused by Phase II. Overall, these experiments show that, despite the limited plasticity of PCs, TTACIL is capable of benefiting from a larger training dataset.

⑥ Effect of the hyperparameters. In this study, we investigate the influence of iterative adjustments during Phase II, the *test-time model refinement* stage of the TTACIL. The results are summarized in Tab. 5. Increasing the number of test-time iterations resulted in a decrease in performance on both datasets, due to overfitting on low-entropy samples, thereby impairing the model’s generalization [52, 86].

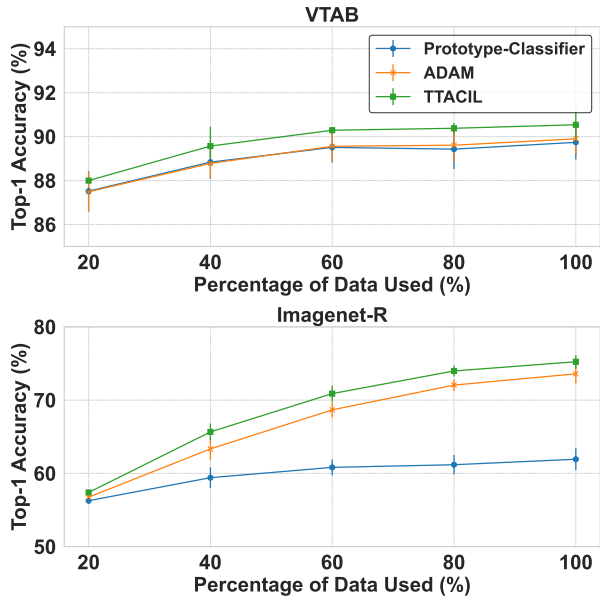


Figure 5. Ablation study on data efficiency. The plots showcase the top-1 accuracy on the VTAB and Imagenet-R datasets with varying percentages of training data used. TTACIL consistently outperforms other methods, especially in lower data regimes, highlighting its robustness to data scarcity.

Overfitting to low-entropy samples, leads to inaccuracies in classifying more complex or higher-entropy samples within the same batch, highlighting a nuanced trade-off between adaptability and overfitting during Phase II.

We also investigated the influence of batch size, number of adaptation iterations, and augmentations per iteration on model performance (see Supp. Mat.).

4.4. Discussion

① Do we really need continuous model updates? A unique element of TTACIL consists of resetting the updated PTM parameters at the end of Phase II. This goes against the conventional practice in CIL where model parameters are continuously updated until the end of all tasks. TTACIL challenges this practice and we show with extensive experiments that state-of-the-art results can be achieved on CIL benchmarks by first session adaptation followed by TTA with a PTM, *without* the need for continuous model updates. We opine that our findings will usher the community to rethink continual model updates while tackling CIL.

② Computational complexity. A drawback of TTA approaches is the increased computational cost during inference. Specifically, in TTACIL, Phase II demands more computation because of the required additional processing before each prediction. This extra computational effort, however, is balanced by a notable improvement in model

Table 5. Summarized results for VTAB and Imagenet-R datasets based on the number of iterations N .

Iterations	VTAB \uparrow	Imagenet-R \uparrow
$N = 1$	90.94 \pm 0.64	78.24 \pm 1.02
$N = 2$	87.34 \pm 3.05	74.77 \pm 1.22
$N = 3$	84.07 \pm 3.53	70.14 \pm 3.35
$N = 4$	80.78 \pm 5.45	69.13 \pm 2.08

plasticity and robustness. Importantly, even with this load, the system can sustain an inference rate of 8 frames/second during a single TTA iteration (see Supp. Mat.).

③ **Practical benefits.** The additional test-time overhead of TTACIL is also balanced by the greater computational efficiency in the training phase, necessitating parameter updates solely on the first task. This contrasts with conventional CIL strategies, which require fine-tuning of PTMs across all tasks [77]. Therefore, our approach leads to a reduction in communication costs when repeatedly disseminating the CIL model to multiple clients in a distributed inference system [50, 51]. Specifically, subsequent tasks necessitate only the transmission of prototypes rather than the entire model in TTACIL.

5. Conclusions

In this work, we show that a minimal adaptation of a PTM, followed by TTA is sufficient to achieve state-of-the-art results on the most common CIL benchmarks. With TTACIL, we bypass repetitive training on each task and directly adapt to the unlabelled test samples during test time. We demonstrated that our method, albeit simpler than many existing state-of-the-art CIL methods, is a promising solution for effective CIL, leveraging large-scale PTMs. It preserves the generalizable representation power of the PTM while being malleable enough to learn new tasks. Additionally, our TTACIL is more robust under common corruptions. This result suggests that in incremental tasks setting, it might not be necessary to perform continual feature learning on all of them: this opens the road to the design of more training-efficient and effective strategies.

Acknowledgements. This paper has been supported by the French National Research Agency (ANR) in the framework of its JCJC, and was funded by the European Union’s Horizon Europe research and innovation program under grant agreement No. 101120237 (ELIAS). Furthermore, this research was partially funded by Hi!PARIS Center on Data Analytics and Artificial Intelligence. This work was granted access to the HPC resources of IDRIS under the allocation AD011013860 made by GENCI.

References

- [1] Amit Alfassy, Assaf Arbelle, Oshri Halimi, Sivan Harary, Roei Herzig, Eli Schwartz, Rameswar Panda, Michele Dolfi, Christoph Auer, Peter Staar, et al. Feta: Towards specializing foundational models for expert task applications. *Adv. Neural Inform. Process. Syst.*, 2022. 4
- [2] Rahaf Aljundi, Francesca Babiloni, Mohamed Elhoseiny, Marcus Rohrbach, and Tinne Tuytelaars. Memory aware synapses: Learning what (not) to forget. In *Eur. Conf. Comput. Vis.*, 2018. 2
- [3] Jimmy Lei Ba, Jamie Ryan Kiros, and Geoffrey E. Hinton. Layer normalization, 2016. 2, 5, 7
- [4] Alexander Bartler, Andre Bühler, Felix Wiewel, Mario Döbler, and Bin Yang. Mt3: Meta test-time training for self-supervised test-time adaptation. In *ICAIC*. PMLR, 2022. 3
- [5] Eden Belouadah, Adrian Popescu, and Ioannis Kanellos. A comprehensive study of class incremental learning algorithms for visual tasks. *Neural Networks*, 135, 2021. 2
- [6] Pietro Buzzega, Matteo Boschini, Angelo Porrello, Davide Abati, and Simone Calderara. Dark experience for general continual learning: a strong, simple baseline. *Adv. Neural Inform. Process. Syst.*, 33, 2020. 3
- [7] Mathilde Caron, Hugo Touvron, Ishan Misra, Hervé Jégou, Julien Mairal, Piotr Bojanowski, and Armand Joulin. Emerging properties in self-supervised vision transformers. In *Int. Conf. Comput. Vis.*, 2021. 7, 4
- [8] Francisco M Castro, Manuel J Marín-Jiménez, Nicolás Guil, Cordelia Schmid, and Karteek Alahari. End-to-end incremental learning. In *Eur. Conf. Comput. Vis.*, 2018. 3
- [9] Arslan Chaudhry, Puneet K Dokania, Thalayasingam Ajathan, and Philip HS Torr. Riemannian walk for incremental learning: Understanding forgetting and intransigence. In *Eur. Conf. Comput. Vis.*, 2018. 2, 3
- [10] Dian Chen, Dequan Wang, Trevor Darrell, and Sayna Ebrahimi. Contrastive test-time adaptation. In *IEEE Conf. Comput. Vis. Pattern Recog.*, 2022. 3
- [11] Shoufa Chen, GE Chongjian, Zhan Tong, Jiangliu Wang, Yibing Song, Jue Wang, and Ping Luo. Adaptformer: Adapting vision transformers for scalable visual recognition. In *Adv. Neural Inform. Process. Syst.*, 2022. 2, 3, 4, 5, 6
- [12] Xiangning Chen, Cho-Jui Hsieh, and Boqing Gong. When vision transformers outperform resnets without pre-training or strong data augmentations. In *Int. Conf. Learn. Represent.*, 2022. 7, 4
- [13] Jia Deng, Wei Dong, Richard Socher, Li-Jia Li, Kai Li, and Li Fei-Fei. Imagenet: A large-scale hierarchical image database. In *IEEE Conf. Comput. Vis. Pattern Recog.*, 2009. 1, 4
- [14] Prithviraj Dhar, Rajat Vikram Singh, Kuan-Chuan Peng, Ziyang Wu, and Rama Chellappa. Learning without memorizing. In *IEEE Conf. Comput. Vis. Pattern Recog.*, 2019. 3
- [15] Alexey Dosovitskiy, Lucas Beyer, Alexander Kolesnikov, Dirk Weissenborn, Xiaohua Zhai, Thomas Unterthiner, Mostafa Dehghani, Matthias Minderer, Georg Heigold, Sylvain Gelly, Jakob Uszkoreit, and Neil Houlsby. An image is

- worth 16x16 words: Transformers for image recognition at scale. In *Int. Conf. Learn. Represent.*, 2021. 1, 3, 5
- [16] Arthur Douillard, Matthieu Cord, Charles Ollion, Thomas Robert, and Eduardo Valle. Podnet: Pooled outputs distillation for small-tasks incremental learning. In *Eur. Conf. Comput. Vis.*, 2020. 3
- [17] Sayna Ebrahimi, Franziska Meier, Roberto Calandra, Trevor Darrell, and Marcus Rohrbach. Adversarial continual learning. In *Eur. Conf. Comput. Vis.*, 2020. 5
- [18] François Fleuret et al. Test time adaptation through perturbation robustness. In *Adv. Neural Inform. Process. Syst. Worksh.*, 2021. 4
- [19] Robert M French. Catastrophic forgetting in connectionist networks. *Trends in cognitive sciences*, 3(4), 1999. 1, 2
- [20] Heitor Murilo Gomes, Jean Paul Barddal, Fabrício Enembreck, and Albert Bifet. A survey on ensemble learning for data stream classification. *CSUR*, 50(2), 2017. 1
- [21] Yves Grandvalet and Yoshua Bengio. Semi-supervised learning by entropy minimization. *Adv. Neural Inform. Process. Syst.*, 17, 2004. 3, 5
- [22] Kaiming He, Xiangyu Zhang, Shaoqing Ren, and Jian Sun. Deep residual learning for image recognition. In *IEEE Conf. Comput. Vis. Pattern Recog.*, 2015. 1
- [23] Kaiming He, Xinlei Chen, Saining Xie, Yanghao Li, Piotr Dollár, and Ross Girshick. Masked autoencoders are scalable vision learners. In *IEEE Conf. Comput. Vis. Pattern Recog.*, 2022. 7, 4
- [24] Dan Hendrycks and Thomas Dietterich. Benchmarking neural network robustness to common corruptions and perturbations. *Int. Conf. Learn. Represent.*, 2019. 2, 3, 5, 6, 1
- [25] Dan Hendrycks, Steven Basart, Norman Mu, Saurav Kadavath, Frank Wang, Evan Dorundo, Rahul Desai, Tyler Zhu, Samyak Parajuli, Mike Guo, et al. The many faces of robustness: A critical analysis of out-of-distribution generalization. In *Int. Conf. Comput. Vis.*, 2021. 5
- [26] Dan Hendrycks, Kevin Zhao, Steven Basart, Jacob Steinhardt, and Dawn Song. Natural adversarial examples. In *IEEE Conf. Comput. Vis. Pattern Recog.*, 2021. 4, 5
- [27] Geoffrey Hinton, Oriol Vinyals, and Jeff Dean. Distilling the knowledge in a neural network. *arXiv preprint arXiv:1503.02531*, 2015. 3, 5
- [28] Saihui Hou, Xinyu Pan, Chen Change Loy, Zilei Wang, and Dahua Lin. Learning a unified classifier incrementally via rebalancing. In *IEEE Conf. Comput. Vis. Pattern Recog.*, 2019. 3
- [29] Neil Houlsby, Andrei Giurgiu, Stanislaw Jastrzebski, Bruna Morrone, Quentin De Laroussilhe, Andrea Gesmundo, Mona Attariyan, and Sylvain Gelly. Parameter-efficient transfer learning for nlp. In *Int. Conf. Mach. Learn.*, 2019. 3, 4
- [30] Paul Janson, Wenxuan Zhang, Rahaf Aljundi, and Mohamed Elhoseiny. A simple baseline that questions the use of pretrained-models in continual learning. In *CVPR Workshop on Distribution Shifts*, 2022. 3
- [31] Menglin Jia, Luming Tang, Bor-Chun Chen, Claire Cardie, Serge J. Belongie, Bharath Hariharan, and Ser-Nam Lim. Visual prompt tuning. In *Eur. Conf. Comput. Vis.*, 2022. 3
- [32] Heechul Jung, Jeongwoo Ju, Minju Jung, and Junmo Kim. Less-forgetting learning in deep neural networks. *arXiv preprint arXiv:1607.00122*, 2016. 3
- [33] Alexander Kirillov, Eric Mintun, Nikhila Ravi, Hanzi Mao, Chloe Rolland, Laura Gustafson, Tete Xiao, Spencer Whitehead, Alexander C. Berg, Wan-Yen Lo, Piotr Dollár, and Ross B. Girshick. Segment anything. *Int. Conf. Comput. Vis.*, 2023. 1
- [34] James Kirkpatrick, Razvan Pascanu, Neil Rabinowitz, Joel Veness, Guillaume Desjardins, Andrei A Rusu, Kieran Milan, John Quan, Tiago Ramalho, Agnieszka Grabska-Barwinska, et al. Overcoming catastrophic forgetting in neural networks. *PNAS*, 114(13), 2017. 3, 5
- [35] Alex Krizhevsky, Geoffrey Hinton, et al. Learning multiple layers of features from tiny images, 2009. 5
- [36] Ananya Kumar, Aditi Raghunathan, Robbie Matthew Jones, Tengyu Ma, and Percy Liang. Fine-tuning can distort pretrained features and underperform out-of-distribution. In *Int. Conf. Learn. Represent.*, 2022. 4
- [37] Janghyeon Lee, Hyeong Gwon Hong, Donggyu Joo, and Junmo Kim. Continual learning with extended kronecker-factored approximate curvature. In *IEEE Conf. Comput. Vis. Pattern Recog.*, 2020. 3
- [38] Zhizhong Li and Derek Hoiem. Learning without forgetting. *IEEE Trans. Pattern Anal. Mach. Intell.*, 2017. 3, 6, 5
- [39] Jian Liang, Ran He, and Tieniu Tan. A comprehensive survey on test-time adaptation under distribution shifts. *arXiv preprint arXiv:2303.15361*, 2023. 2, 3
- [40] Xialei Liu, Marc Masana, Luis Herranz, Joost Van de Weijer, Antonio M Lopez, and Andrew D Bagdanov. Rotate your networks: Better weight consolidation and less catastrophic forgetting. In *ICPR*, 2018. 3
- [41] Yaoyao Liu, Yuting Su, An-An Liu, Bernt Schiele, and Qianru Sun. Mnemonics training: Multi-class incremental learning without forgetting. In *IEEE Conf. Comput. Vis. Pattern Recog.*, 2020. 3
- [42] Yuejiang Liu, Parth Kothari, Bastien van Delft, Baptiste Bellot-Gurlet, Taylor Mordan, and Alexandre Alahi. Ttt++: When does self-supervised test-time training fail or thrive? *Adv. Neural Inform. Process. Syst.*, 2021. 3
- [43] Zheda Mai, Ruiwen Li, Hyunwoo Kim, and Scott Sanner. Supervised contrastive replay: Revisiting the nearest class mean classifier in online class-incremental continual learning. In *IEEE Conf. Comput. Vis. Pattern Recog.*, 2021. 4
- [44] Arun Mallya and Svetlana Lazebnik. Packnet: Adding multiple tasks to a single network by iterative pruning. In *IEEE Conf. Comput. Vis. Pattern Recog.*, 2018. 3
- [45] Arun Mallya, Dillon Davis, and Svetlana Lazebnik. Piggyback: Adapting a single network to multiple tasks by learning to mask weights. In *Eur. Conf. Comput. Vis.*, 2018. 3
- [46] Imad Eddine Marouf, Enzo Tartaglione, and Stéphane Lathuilière. Mini but mighty: Finetuning vits with mini adapters. In *Proceedings of the IEEE/CVF Winter Conference on Applications of Computer Vision*, 2024. 3
- [47] Marc Masana, Xialei Liu, Bartłomiej Twardowski, Mikel Menta, Andrew D Bagdanov, and Joost van de Weijer. Class-incremental learning: survey and performance evaluation on

- image classification. *IEEE Trans. Pattern Anal. Mach. Intell.*, 2022. 1, 2
- [48] Thomas Mensink, Jakob Verbeek, Florent Perronnin, and Gabriela Csurka. Distance-based image classification: Generalizing to new classes at near-zero cost. *IEEE Trans. Pattern Anal. Mach. Intell.*, 2013. 2, 3
- [49] Martial Mermillod, Aurélie Bugaïska, and Patrick Bonin. The stability-plasticity dilemma: Investigating the continuum from catastrophic forgetting to age-limited learning effects. *Frontiers in psychology*, 4:504, 2013. 2
- [50] Mohammad Hasanzadeh Mofrad, Rami Melhem, Yousuf Ahmad, and Mohammad Hammoud. Accelerating distributed inference of sparse deep neural networks via mitigating the straggler effect. In *2020 IEEE High Performance Extreme Computing Conference (HPEC)*, pages 1–7, 2020. 9
- [51] Thaha Mohammed, Carlee Joe-Wong, Rohit Babbar, and Mario Di Francesco. Distributed inference acceleration with adaptive dnn partitioning and offloading. In *IEEE INFOCOM 2020 - IEEE Conference on Computer Communications*, 2020. 9
- [52] Shuaicheng Niu, Jiayang Wu, Yifan Zhang, Yafo Chen, Shijian Zheng, Peilin Zhao, and Mingkui Tan. Efficient test-time model adaptation without forgetting. In *Int. Conf. Mach. Lear.* PMLR, 2022. 5, 8, 1
- [53] Shuaicheng Niu, Jiayang Wu, Yifan Zhang, Zhiquan Wen, Yafo Chen, Peilin Zhao, and Mingkui Tan. Towards stable test-time adaptation in dynamic wild world. In *Int. Conf. Learn. Represent.*, 2023. 7
- [54] Oleksiy Ostapenko, Mihai Puscas, Tassilo Klein, Patrick Jah-nichen, and Moin Nabi. Learning to remember: A synaptic plasticity driven framework for continual learning. In *IEEE Conf. Comput. Vis. Pattern Recog.*, 2019. 3
- [55] Aristeidis Panos, Yuriko Kobe, Daniel Olmeda Reino, Rahaf Aljundi, and Richard E Turner. First session adaptation: A strong replay-free baseline for class-incremental learning. In *Int. Conf. Comput. Vis.*, 2023. 2, 3, 5, 6
- [56] German I Parisi, Ronald Kemker, Jose L Part, Christopher Kanan, and Stefan Wermter. Continual lifelong learning with neural networks: A review. *Neural Networks*, 113, 2019. 2
- [57] Xingchao Peng, Ben Usman, Neela Kaushik, Judy Hoffman, Dequan Wang, and Kate Saenko. Visda: The visual domain adaptation challenge. *arXiv preprint arXiv:1710.06924*, 2017. 3
- [58] Ameya Prabhu, Philip HS Torr, and Puneet K Dokania. Gdumb: A simple approach that questions our progress in continual learning. In *Eur. Conf. Comput. Vis.*, 2020. 3
- [59] Ameya Prabhu, Hasan Abed Al Kader Hammoud, Puneet K Dokania, Philip HS Torr, Ser-Nam Lim, Bernard Ghanem, and Adel Bibi. Computationally budgeted continual learning: What does matter? In *IEEE Conf. Comput. Vis. Pattern Recog.*, 2023. 7
- [60] Joaquin Quinonero-Candela, Masashi Sugiyama, Anton Schwaighofer, and Neil D Lawrence. *Dataset shift in machine learning*. Mit Press, 2008. 2
- [61] Alec Radford, Jong Wook Kim, Chris Hallacy, Aditya Ramesh, Gabriel Goh, Sandhini Agarwal, Girish Sastry, Amanda Askell, Pamela Mishkin, Jack Clark, et al. Learning transferable visual models from natural language supervision. In *Int. Conf. Mach. Lear.*, 2021. 7, 8, 4
- [62] Sylvestre-Alvise Rebuffi, Alexander Kolesnikov, Georg Sperl, and Christoph H Lampert. icarl: Incremental classifier and representation learning. In *IEEE Conf. Comput. Vis. Pattern Recog.*, 2017. 3, 5
- [63] Tal Ridnik, Emanuel Ben-Baruch, Asaf Noy, and Lihi Zelnik-Manor. Imagenet-21k pretraining for the masses, 2021. 3
- [64] Andrei A Rusu, Neil C Rabinowitz, Guillaume Desjardins, Hubert Soyer, James Kirkpatrick, Koray Kavukcuoglu, Razvan Pascanu, and Raia Hadsell. Progressive neural networks. *arXiv preprint arXiv:1606.04671*, 2016. 3
- [65] Jonathan Schwarz, Wojciech Czarnecki, Jelena Luketina, Agnieszka Grabska-Barwinska, Yee Whye Teh, Razvan Pascanu, and Raia Hadsell. Progress & compress: A scalable framework for continual learning. In *Int. Conf. Mach. Lear.*, 2018. 3
- [66] Hanul Shin, Jung Kwon Lee, Jaehong Kim, and Jiwon Kim. Continual learning with deep generative replay. *Adv. Neural Inform. Process. Syst.*, 2017. 3
- [67] James Seale Smith, Leonid Karlinsky, Vyshnavi Gutta, Paola Cascante-Bonilla, Donghyun Kim, Assaf Arbelle, Rameswar Panda, Rogerio Feris, and Zsolt Kira. Coda-prompt: Continual decomposed attention-based prompting for rehearsal-free continual learning. In *IEEE Conf. Comput. Vis. Pattern Recog.*, 2023. 3
- [68] Junha Song, Jungsoo Lee, In So Kweon, and Sungha Choi. Ecotta: Memory-efficient continual test-time adaptation via self-distilled regularization. In *IEEE Conf. Comput. Vis. Pattern Recog.*, 2023. 3
- [69] Yu Sun, Xiaolong Wang, Zhuang Liu, John Miller, Alexei Efros, and Moritz Hardt. Test-time training with self-supervision for generalization under distribution shifts. In *Int. Conf. Mach. Lear.*, 2020. 3, 4
- [70] Mingxing Tan, Ruoming Pang, and Quoc V Le. Efficientdet: Scalable and efficient object detection. In *IEEE Conf. Comput. Vis. Pattern Recog.*, 2020. 1
- [71] Andrés Villa, Juan León Alcázar, Motasem Alfarra, Kumail Alhamoud, Julio Hurtado, Fabian Caba Heilbron, Alvaro Soto, and Bernard Ghanem. Pivot: Prompting for video continual learning. In *IEEE Conf. Comput. Vis. Pattern Recog.*, 2023. 1, 3
- [72] C. Wah, S. Branson, P. Welinder, P. Perona, and S. Belongie. The Caltech-UCSD Birds-200-2011 Dataset. Technical Report CNS-TR-2011-001, California Institute of Technology, 2011. 5
- [73] Dequan Wang, Evan Shelhamer, Shaoteng Liu, Bruno Olshausen, and Trevor Darrell. Tent: Fully test-time adaptation by entropy minimization. In *Int. Conf. Learn. Represent.*, 2021. 3, 4, 7
- [74] Liyuan Wang, Xingxing Zhang, Hang Su, and Jun Zhu. A comprehensive survey of continual learning: Theory, method and application, 2023. 1, 2
- [75] Qin Wang, Olga Fink, Luc Van Gool, and Dengxin Dai. Continual test-time domain adaptation. In *IEEE Conf. Comput. Vis. Pattern Recog.*, 2022. 3

- [76] Yabin Wang, Zhiwu Huang, and Xiaopeng Hong. S-prompts learning with pre-trained transformers: An occam’s razor for domain incremental learning. *Adv. Neural Inform. Process. Syst.*, 35, 2022. 1
- [77] Zifeng Wang, Zizhao Zhang, Sayna Ebrahimi, Ruoxi Sun, Han Zhang, Chen-Yu Lee, Xiaoqi Ren, Guolong Su, Vincent Perot, Jennifer Dy, et al. Dualprompt: Complementary prompting for rehearsal-free continual learning. In *Eur. Conf. Comput. Vis.*, 2022. 2, 3, 5, 6, 7, 9, 4
- [78] Zifeng Wang, Zizhao Zhang, Chen-Yu Lee, Han Zhang, Ruoxi Sun, Xiaoqi Ren, Guolong Su, Vincent Perot, Jennifer Dy, and Tomas Pfister. Learning to prompt for continual learning. In *IEEE Conf. Comput. Vis. Pattern Recog.*, 2022. 1, 2, 3, 5, 6, 4
- [79] Ross Wightman. Pytorch image models. <https://github.com/rwightman/pytorch-image-models>, 2019. 4
- [80] Ye Xiang, Ying Fu, Pan Ji, and Hua Huang. Incremental learning using conditional adversarial networks. In *Int. Conf. Comput. Vis.*, 2019. 3
- [81] Friedemann Zenke, Ben Poole, and Surya Ganguli. Continual learning through synaptic intelligence. In *Int. Conf. Mach. Lear.*, 2017. 3
- [82] Xiaohua Zhai, Joan Puigcerver, Alexander Kolesnikov, Pierre Ruyssen, Carlos Riquelme, Mario Lucic, Josip Djolonga, Andre Susano Pinto, Maxim Neumann, Alexey Dosovitskiy, et al. A large-scale study of representation learning with the visual task adaptation benchmark. *arXiv preprint arXiv:1910.04867*, 2019. 5
- [83] Gengwei Zhang, Liyuan Wang, Guoliang Kang, Ling Chen, and Yunchao Wei. Slca: Slow learner with classifier alignment for continual learning on a pre-trained model. In *Int. Conf. Comput. Vis.*, 2023. 3, 5, 6
- [84] Marvin Mengxin Zhang, Sergey Levine, and Chelsea Finn. Memo: Test time robustness via adaptation and augmentation. In *NeurIPS 2021 Workshop on Distribution Shifts: Connecting Methods and Applications*, 2021. 2, 3, 4, 5, 7
- [85] Yuanhan Zhang, Zhenfei Yin, Jing Shao, and Ziwei Liu. Benchmarking omni-vision representation through the lens of visual realms. In *Eur. Conf. Comput. Vis.* Springer, 2022. 5
- [86] Hao Zhao, Yuejiang Liu, Alexandre Alahi, and Tao Lin. On pitfalls of test-time adaptation, 2023. 7, 8
- [87] Da-Wei Zhou, Han-Jia Ye, and De-Chuan Zhan. Co-transport for class-incremental learning. In *ACM MM*, 2021. 5
- [88] Da-Wei Zhou, Qi-Wei Wang, Zhi-Hong Qi, Han-Jia Ye, De-Chuan Zhan, and Ziwei Liu. Deep class-incremental learning: A survey. *arXiv preprint arXiv:2302.03648*, 2023. 2
- [89] Da-Wei Zhou, Han-Jia Ye, De-Chuan Zhan, and Ziwei Liu. Revisiting class-incremental learning with pre-trained models: Generalizability and adaptivity are all you need, 2023. 1, 2, 3, 5, 6, 7, 4
- [90] Kaiyang Zhou, Jingkang Yang, Chen Change Loy, and Ziwei Liu. Learning to prompt for vision-language models. *Int. Conf. Comput. Vis.*, 2022. 3

Rethinking Class-incremental Learning in the Era of Large Pre-trained Models via Test-Time Adaptation

Supplementary Material

In this supplementary material, we provide more details about the experimental results mentioned in the main paper, as well as additional empirical evaluations and discussions. The supplementary material is organized as follows: In Section **A**, we evaluate the effect of task order. Section **B** provides additional evaluations on CIFAR100-C dataset. Section **C** reports the full ablation studies in the main paper. In Section **E**, we analyze the training and inference cost of TTACIL. Section **G** provides an ablation study about the Adapter size in TTACIL. In Section **H**, we detail the baselines, and datasets used in our experiments.

A. Effect of Varying Task Sequence Orders

This section evaluates the adaptability of our proposed method TTACIL and compares it with ADAM in CIL scenarios on the 5-Datasets benchmark. We specifically delve deeper into the experiments discussed in Sec. 4.3 of the main paper, where we analyze the influence of task order on the impact of the task order. We provide more detailed experimental results considering multiple task orders. The task sequences include variations with SVHN, MNIST, CIFAR10, NotMNIST, and FashionMNIST. Results are reported in Tab. 6. The orange cells corresponding to the first task, both ADAM and TTACIL have been trained on.

The results indicate the substantial influence of task sequence on model performance, highlighting the pivotal role of the initial task. TTACIL consistently surpasses ADAM in all sequences, with a maximum performance gain of +10.29% observed in the SVHN → MNIST → CIFAR10 → NotMNIST → FashionMNIST sequence. This suggests that TTACIL effectively leverages unlabeled data from subsequent tasks to improve its adaptability.

B. Evaluation on CIFAR100-C with Level-5 Corruptions

We compare our method, TTACIL, with state-of-the-art methods on CIFAR100-C with Level-5 corruptions [24], as summarized in Tab. 7. The Prototype-Classifier performs poorly, yielding a 53.89% average accuracy, due to its reliance on pre-trained representations. ADAM improves upon this with a 66.57% average accuracy, courtesy of its initial task training.

In contrast, TTACIL achieves the highest average accuracy of 68.00%, outperforming ADAM by a significant margin of +5.13% on CIFAR100-C. These results substantiate TTACIL’s superior adaptability and robustness to a

variety of corruptions.

C. Ablation Study: Augmentations, Iterations, and Batch Size

Effect of the batch size. We ablate the effect of varying the batch size on the final performance in Tab. 8. Our findings, averaged over these 3 seeds, reveal a complex relationship between batch size and model performance. Specifically, performance on the “VTAB” dataset reaches about 90% when the batch size approaches 4 and remains almost constant for larger batch sizes. On the contrary, we observe an important decrease in performance on the Imagenet-R dataset when increasing the batch size. This behavior could be potentially explained by a mix of both low and high-entropy samples that could adversely affect TTA [52].

Effect of the number of adaptation iterations. In this study our goal is to quantify the influence of iterative adjustments during Phase II, the *test-time refinement* stage of the TTACIL. The results are summarized in Tab. 5. The results show that the performance decreases when increasing the number of test-time iterations on both datasets. Specifically, performance on VTAB descends from an initial 90.55% with one iteration to 80.78% at four iterations. A congruent decrement is observed in Imagenet-R, where the accuracy declines from 75.05% to 69.13% as the iteration count is augmented.

This performance drop may be due to the model’s propensity for overfitting to low-entropy samples as discussed in [52]. Although this overconfidence enhances the model’s accuracy in these specific instances, it undermines its broader generalization capabilities. This leads to inaccuracies in classifying more complex or higher-entropy samples within the same batch, highlighting a nuanced trade-off between adaptability and overfitting during the test-time adjustment phase.

Effect of the number of Augmentations per adaptation iteration. We analyze the effect of varying the set of augmentations used in the TTA phase. We report the final performance in Tab. 10 using a varying number of augmentations, where the results are aggregated across the 3 seeds. They show that TTACIL consistently maintains a high accuracy across both the VTAB and Imagenet-R datasets. It is important to mention that while increasing the number of augmentations may seem advantageous, it introduces additional computational overhead during inference, warranting careful consideration. Thus, it is recommended to keep a small number of augmentations in the range of

Table 6. Performance Comparison of ADAM [89] and TTACIL. Across Varying Task Sequence Orders in Class-Incremental Learning. Top-1 accuracy is reported (\uparrow). Orange cells indicate the task that the model has been trained on. The model used in ViT-B/16 pre-trained on Imagenet-21K.

Method		SVHN	MNIST	CIFAR10	NotMNIST	FashionMNIST	Average
Prototype-Classifier		33.18	83.78	95.63	68.85	83.18	72.92
ADAM [89]	SVHN	33.44	83.84	95.62	68.85	83.14	72.98
	MNIST	92.44	93.95	72.77	83.00	40.22	76.48
	CIFAR10	97.24	67.97	83.63	31.33	84.04	72.84
	NotMNIST	71.02	83.66	38.20	86.51	95.89	75.06
	FashionMNIST	84.19	31.52	85.69	95.96	69.93	73.46
Ours	SVHN	95.13	96.48	67.33	78.43	78.96	83.27
	MNIST	97.89	76.15	82.35	83.09	53.28	78.55
	CIFAR10	98.95	70.37	83.24	35.03	82.19	73.96
	NotMNIST	88.67	83.82	59.16	92.76	73.61	<u>79.60</u>
	FashionMNIST	91.02	44.35	84.63	82.50	77.78	76.06

Table 7. Average and last performance comparison on seven datasets with ViT-B/16-IN21K as the backbone on CIFAR100-C with Level-5 corruptions [24]. The best performance is shown in bold, and the second best is underlined.

Method	Noise			Blur				Weather			Average	
	Gauss.	Shot	Impul.	Defoc.	Glass	Motion	Zoom	Snow	Frost	Fog		Brit.
Prototype-Classifier	35.52	39.05	46.89	59.78	31.29	56.99	65.04	64.41	63.99	50.13	79.68	53.89
ADAM [89]	37.52	48.73	65.03	78.02	39.80	74.59	79.27	76.92	73.34	70.50	88.59	<u>66.57</u>
TTACIL	47.33	51.45	67.89	78.52	42.70	75.00	79.00	75.31	72.49	69.20	89.09	68.00

Table 8. Summarized results for VTAB and Imagenet-R datasets on the effect of batch size B in TTACIL. (Mean \pm Std. Dev.)

Batch Size (B)	VTAB \uparrow	Imagenet-R \uparrow
1	88.14 \pm 1.71	79.11 \pm 1.46
4	89.81 \pm 2.62	<u>78.22</u> \pm 2.54
8	88.91 \pm 2.87	78.24 \pm 1.02
16	90.94 \pm 0.64	75.26 \pm 0.85
32	<u>90.31</u> \pm 0.09	69.12 \pm 0.60

Table 9. Summarized results for VTAB and Imagenet-R datasets based on the number of iterations N . (Mean \pm Std. Dev.)

Iterations	VTAB \uparrow	Imagenet-R \uparrow
$N = 1$	90.94 \pm 0.64	78.24 \pm 1.02
$N = 2$	<u>87.34</u> \pm 3.05	<u>74.77</u> \pm 1.22
$N = 3$	84.07 \pm 3.53	70.14 \pm 3.35
$N = 4$	80.78 \pm 5.45	69.13 \pm 2.08

$M \in [1, \dots, 8]$ since the performance of TTACIL does not benefit significantly from large M .

Table 10. Summarized results for VTAB and Imagenet-R datasets based on the number of augmentations M . (Mean \pm Std. Dev.)

Augmentations (M)	VTAB \uparrow	Imagenet-R \uparrow
4	90.14 \pm 0.72	75.30 \pm 0.87
8	<u>90.11</u> \pm 0.34	75.22 \pm 0.91
16	90.94 \pm 0.64	75.26 \pm 0.85
24	90.11 \pm 0.46	<u>75.23</u> \pm 0.80

D. Data Efficiency

This section presents the results of the ablation study conducted in Sec. 4.3 of the main paper, which focuses on the data efficiency of our method TTACIL. Tab. 11 details the results presented in Fig. 4 in the main paper.

The study aims to examine how well TTACIL performs under varying degrees of data scarcity for training. We compare TTACIL’s performance against state-of-the-art methods like Prototype-classifier and ADAM across different datasets including VTAB and Imagenet-R.

Table 11. Performance comparison under varying data scarcity for training.

Training Data (%)	Prototype-classifier		ADAM		TTACIL (Ours)	
	VTAB	Imagenet-R	VTAB	Imagenet-R	VTAB	Imagenet-R
20%	87.52 ± 0.91	56.27 ± 0.45	87.49 ± 0.91	56.75 ± 0.40	88.00 ± 0.03	57.39 ± 0.29
40%	88.84 ± 0.76	59.41 ± 1.42	88.78 ± 0.66	63.34 ± 1.51	89.57 ± 0.88	65.66 ± 1.15
60%	89.51 ± 0.69	60.82 ± 1.10	89.56 ± 0.71	68.67 ± 1.08	90.29 ± 0.14	70.89 ± 1.09
80%	89.43 ± 0.90	61.18 ± 1.32	89.61 ± 0.75	72.05 ± 0.82	90.38 ± 0.24	73.98 ± 0.75
100%	89.74 ± 0.78	61.93 ± 1.49	89.90 ± 0.67	73.59 ± 1.34	90.54 ± 0.64	75.26 ± 0.80

E. Training and Inference cost

Training Cost. Contrasting to traditional methods that necessitate training on each task’s data, TTACIL employs PTMs and focuses on fine-tuning a minimal subset of parameters, specifically *Adapters* which constitute merely 1.4% of the total parameter count (only 1.2M for ViT-B/16). This approach yields substantial benefits in training efficiency. Firstly, TTACIL demands training solely on the initial task, substantially curtailing the computational load relative to methods requiring retraining for every new class or task. Secondly, the method’s parameter efficiency is noteworthy, minimizing the need for extensive computational resources while still delivering high performance.

Table 12. Training specifications comparison between TTACIL and SLCA on Imagenet-R using ViT-B/16 [15].

Methods	Param.	Train.	Epochs	Time (s)
SLCA [83]	87M	100%	20	2440
TTACIL (Ours)	1.2M	1.4%	20	75

Unlike, other approaches such as SLCA [83], which fine-tunes all the parameters of the PTM (see Tab. 12, or by introducing a high number of trainable parameters to the initial backbones such as L2P [78], DualPrompt [77] (2.4M for ViT-B/16). Tab. 12 shows that TTACIL reduces the training time by 32X times compared to SLCA due to parameter efficiency, and finetuning only on the first task. Additionally, TTACIL training cost does not grow linearly with the number of tasks as traditional CIL methods.

Inference Cost. In TTACIL, we introduce extra computation with an added optimization step before prediction, we now delve into a detailed analysis of the inference cost associated with TTACIL. By quantifying the inference time, we compare our method with two baselines: ADAM and Prototype-Classifer. Concretely, in TTACIL the inference time accounts for both TTA optimization and final prediction. We report the inference time (in milliseconds) averaged over five runs on an A100 (48GB) GPU. Our evaluation for TTACIL, we use one iteration $N = 1$, with $M = 8$ of augmentations.

Table 13. Inference Time Comparison in Milliseconds (ms). The results are an average of 5 runs. GFLOPS/GMACs are evaluated on batch-size $B = 16$.

Batch Size	TTACIL	Prototype-Classifer	ADAM
$B = 1$	220	17	<u>22</u>
$B = 4$	550	18	<u>23</u>
$B = 8$	930	17	23
$B = 16$	1820	22	27
$B = 24$	2700	31	34
GFLOPS	85.45	33.72	<u>34.18</u>
GMACs	42.73	16.86	<u>17.09</u>

The computational overhead introduced by TTACIL is a trade-off for enhanced model plasticity and robustness. This increased computational cost during inference is offset by the method’s efficiency during training, where only the Layer Normalization parameters are updated in the initial task.

Tab. 14 quantifies the inference time of TTACIL across varying batch sizes B and adaptation iterations N . The results emphasize the computational trade-offs involved in choosing different hyperparameters for TTACIL. It’s noteworthy that the rate of increase in execution time is not as steep when transitioning to larger batch sizes compared to smaller ones.

For instance, when comparing $B = 1$ to $B = 4$ at $N = 1$, the execution time goes from 190 ms to 470 ms, an increase of 280 ms. However, the increase is less pronounced when the batch size goes from $B = 8$ to $B = 16$; the time for $N = 1$ only increases by 770 ms, from 1000 ms to 1770 ms. This suggests that TTACIL demonstrates a form of computational efficiency with larger batch sizes in terms of execution time per unit increase in batch size.

In CIL, approaches like L2P [78] and DualPrompt [77] have demonstrated considerable proficiency in mitigating catastrophic forgetting. They achieve this by utilizing step-specific keys and activations from PTMs to selectively utilize prompts during each inference task. However, these methods come with certain limitations, particularly in terms

Table 14. Execution Time comparison in milliseconds (ms) concerning the number of adaptation iterations N /batch-size B .

		Iterations			
		$N = 1$	$N = 2$	$N = 3$	$N = 4$
Batch-size	$B = 1$	190	<u>250</u>	320	340
	$B = 4$	470	630	680	810
	$B = 8$	1000	1110	1270	1410
	$B = 16$	1770	2140	2480	2460

of computational efficiency during the inference stage. The primary factor contributing to this increased computational demand is the prompt selection mechanism, which necessitates additional processing to determine the most suitable prompts for each specific inference task. Additionally, the integration of these prompts leads to an expansion of the embedding space within the PTM, further adding to the computational load.

While these methods exhibit increased computational costs during inference, it is important to note that our approach, TTACIL, also entails an elevation in inference costs. However, the nature of this increase is distinct. In TTACIL, the enhanced computational demand is primarily due to the test-time adaptation process, which involves fine-tuning a subset of parameters for each new task. Despite this, TTACIL offers a balanced approach by reducing the overall training cost and effectively addressing the issue of catastrophic forgetting, distinguishing it from methods like L2P and DualPrompt.

F. Pre-Trained Models

Since there are various kinds of pre-trained models publicly available, we follow [77, 78] to choose the most commonly used ones in the main paper for evaluation, denoted as **ViT-B/16-IN1K** and **ViT-B/16-IN21K**. Specifically, both models are pre-trained on ImageNet21K [13], while ViT-B/16-IN1K is further finetuned with ImageNet1K. We follow timm [79] implementation and report the details about these models in Tab. 15. We report the backbones adopted in the ablation study, including ViT-L/16-IN1K, ViT-B/16-DINO [7], ViT-B/16-SAM [12], ViT-B/16-MAE [23], ViT-B/16-CLIP [61] (image encoder), in the table. Among them, ViT-B/16-DINO and ViT-B/16-MAE are trained with self-supervised loss, and ViT-B/16-CLIP is trained on 400 million image-text pairs with contrastive loss.

G. Adapter

The Adapter module, a bottleneck structure extensively studied in prior works [11, 29], enables fine-tuning of Vision Transformer (ViT) outputs. Composed of a down-projection $W_{\text{down}} \in \mathbb{R}^{d \times r}$, a non-linear activation function, and an up-projection $W_{\text{up}} \in \mathbb{R}^{r \times d}$, it facilitates dimension-

Table 15. Adopted PTM architectures in the main paper.

Model	# params	Link
ViT-B/16-IN1K	86M	Link
ViT-B/16-IN21K	86M	Link
ViT-L/16-IN1K	303M	Link
ViT-B/16-DINO	86M	Link
ViT-B/16-SAM	86M	Link
ViT-B/16-MAE	86M	Link
ViT-B/16-CLIP	86M	Link

ality reduction and subsequent restoration. We adopt the AdaptMLP structure as introduced in AdaptFormer [11], effectively replacing ViT’s native MLP. Given the input \mathbf{x}_ℓ to the MLP, the output can be expressed as:

$$\text{MLP}(\mathbf{x}_\ell) + s \cdot \text{ReLU}(\mathbf{x}_\ell W_{\text{down}}) W_{\text{up}}, \quad (5)$$

where s is an optional, learnable scaling parameter. As done in ADAM [89], during the adaptation phase, only adapter parameters are optimized, while the pre-trained weights of ViT remain fixed. We employ a hidden dimension r of 16, resulting in approximately 0.3 million tunable parameters, a figure substantially lower than the 86 million parameters in the standard ViT-B/16 model.

Ablation Study on Adapter Sizes in TTACIL. Tab. 16 presents an ablation study examining the effect of varying adapter sizes r on the average performance across multiple datasets such as VTAB, CIFAR100, and ImageNet-R. The reported trainable parameters also scale with the adapter size, giving us an insight into the computational cost involved.

The table reveals that increasing the adapter size does not substantially improve the model’s performance. For instance, while moving from $r = 16$ to $r = 256$, the average accuracy on the VTAB dataset slightly decreases from 89.65% to 88.65%. A similar trend is observed in the CIFAR100 and ImageNet-R datasets, with only marginal performance improvements or even slight deteriorations.

More importantly, the increase in adapter size comes at a substantial computational cost. The number of trainable parameters rises exponentially with the adapter size, going from 0.30 Million for $r = 16$ to 4.73M for $r = 256$. This not only increases the model’s complexity but also makes it computationally expensive to train.

In summary, our analysis underscores the conclusion that while increasing the adapter size in TTACIL may seem like a plausible avenue for performance improvement, it does not offer significant gains. Instead, it introduces computational inefficiencies due to the escalated number of trainable parameters, thereby questioning the trade-off between performance and computational cost.

Table 16. Comparison of TTACIL Average performance Across Different Adapter Sizes r across datasets. The reported number of trainable parameters is in Million (M).

	$r = 16$	$r = 32$	$r = 128$	$r = 256$
Params (M)	0.30	0.60	2.37	4.73
VTAB	89.65	<u>89.18</u>	88.83	88.65
CIFAR100	90.25	<u>90.14</u>	89.25	89.04
ImageNet-R	74.72	<u>75.03</u>	75.39	74.99

H. Baselines

We briefly outline the methods against which our approach is evaluated:

- **Finetune**: Incrementally trains on new datasets, inducing catastrophic forgetting as a consequence.
- **Finetune Adapter** [11]: Retains pre-trained weights while optimizing an adapter module. Classifiers specific to the current dataset D_t are fine-tuned, while those for previous classes are held constant.
- **LwF** [38]: Employs knowledge distillation [27] as a regularizer to mitigate forgetting, relying on the legacy model for soft target generation.
- **L2P** [78]: A leading PTM-based CIL method that maintains a frozen pre-trained model while optimizing a prompt pool. It incorporates a 'key-value' pairing mechanism for prompt selection and leverages an auxiliary pre-trained model for prompt retrieval.
- **DualPrompt** [77]: An extension of L2P that utilizes two categories of prompts—general and expert—for enhanced performance. It also uses an additional pre-trained model for prompt retrieval.
- **FSA-FiLM** [55]: FSA adapts a pre-trained neural network body only on the first learning session and fixes it thereafter; a head based on linear discriminant analysis (LDA), is then placed on top of the adapted body, allowing exact updates through CIL.
- **ADAM** [89]: fine-tunes the adapters [11] only on the first task, among the sequences of all the tasks in a dataset, to adapt to the dataset at hand.
- **SLCA** [83]: improves the classification layer by modeling the class-wise distributions and aligning the classification layers in a post-hoc fashion.

I. Datasets

We describe the datasets utilized in our study, summarized in Tab. 17. While CIFAR100, CUB200, and ImageNet-R are established CIL benchmarks [62, 77, 87], ImageNet is ill-suited for PTM-based CIL evaluation due to data overlap [78]. Consequently, we introduce four additional benchmarks characterized by non-overlap with ImageNet, sub-

Table 17. Introduction about benchmark datasets. ObjectNet, OmniBenchmark, and VTAB contain massive classes, and we sample a subset from them to construct the incremental learning task.

Dataset	# training instances	# testing instances	# Classes	Link
CIFAR100	50,000	10,000	100	Link
CUB200	9,430	2,358	200	Link
ImageNet-R	24,000	6,000	200	Link
ImageNet-A	5,981	1,519	200	Link
ObjectNet	26,509	6,628	200	Link
OmniBenchmark	89,697	5,985	300	Link
VTAB	1,796	8,619	50	Link
5-datasets	180,869	506,906	50	Link

stantial domain diversity, and large-scale, cross-domain instances.

- **CIFAR100** [35]: Comprises 100 classes, 60,000 images—50,000 for training and 10,000 for testing.
- **CUB200** [72]: Focuses on fine-grained visual categorization, containing 11,788 bird images across 200 subcategories, with 9,430 for training and 2,358 for testing.
- **ImageNet-R** [25]: Extended for CIL by [77], includes various styles and hard instances, totaling 24,000 training and 6,000 testing instances.
- **ImageNet-A** [26]: Features real-world adversarially filtered images, with 5,981 training and 1,519 testing instances.
- **OmniBenchmark** [85]: A diverse benchmark challenging PTM generalization, containing 89,697 training and 5,985 testing instances across multiple semantic realms.
- **VTAB** [82]: Encompasses 19 tasks across three categories—Natural, Specialized, and Structured. We select five datasets to construct a cross-domain CIL setting. Similar to ADAM [89], we select 5 to construct a cross-domain class-incremental learning setting, i.e., Resisc45, DTD, Pets, EuroSAT, and Flowers.
- **5-datasets** [17]: a sequence of classification datasets including SVHN, CIFAR10, not-MNIST, Fashion-MNIST and, and MNIST.